Book title

2nd edition

Author Firstname Surname
Author Address
Department of Chemistry
University of Florida

Author Firstname Surname
Author Address

Dedication

Contents

Preface

The ends of words and sentences are marked by spaces. It doesn't matter how many spaces you type; one is as good as 100. The end of a line counts as a space.

The ends of words and sentences are marked by spaces. It doesn't matter how many spaces you type; one is as good as 100. The end of a line counts as a space.

The ends of words and sentences are marked by spaces. It doesn't matter how many spaces you type; one is as good as 100. The end of a line counts as a space.

Name

Biography

SIR STANLEY DAVIDSON (1894–1981)

One or more blank lines denote the end of a paragraph. The ends of words and sentences are marked by spaces. It doesn't matter how many spaces you type; one is as good as 100. The end of a line counts as a space.

Part I

Part title

Chapter 1

A Digital Twin for Part Quality Prediction and Control in Plastic Injection Molding

ABSTRACT

The plastic injection molding process has been established as the most widespread manufacturing process in the plastic processing industry. It is employed by almost 70 % of all plastic processing companies [1, 2]. Among the decisive factors contributing to its prevalence are its ability to manufacture parts with intricate geometries and its high degree of automation. Approaches of varying complexity to control part quality in order to reduce waste and increase the efficiency of the process exist: The industry standard is the control of so-called machine-variables, i.e., process variables that are measured on the machine-side of the process. This does not take into account any variables that reflect the true state of the emerging part. For this reason, the scientific community aims to control process variables that are measured cavity-side, more precisely the pressure in the mold cavity. However, the implementation of pressure control requires significant control knowledge and is not suitable for large-scale industrial application. The objective of this contribution is therefore to transform an ordinary machine-variable controlled injection molding machine to a Cyber Physical Production System (CPPS) via augmentation by a digital twin (DT). The digital twin will predict part quality from process variables. To this end, a state of the art industrial injection molding machine will be equipped with additional sensors that measure in-cavity process variables. Moreover, an in-line quality measuring cell is added. By doing so, all machine, process, and quality data required for data-driven modelling, and perspectively control are acquired. Subsequently, an internal dynamics approach for predicting final batch quality from process value trajectories is proposed and compared to the current state of the art modelling approaches in two case studies.

KEYWORDS

Digital Twin, Plastic Injection Molding, part quality prediction, OPC-UA

1.1 INTRODUCTION

After the first injection molding (IM) machine was patented in 1872 [3], the large scale integration of this processing method into series production started towards the end of the first quarter of the 20th century with the introduction of new polymer materials that allowed more complex part geometries and shorter

processing cycle times. With the invention of screw IM machines in 1946 [4], process parameters such as the injection velocity could be controlled more precisely, resulting in increased qualities of the produced parts. While today piston IM machines are still used for special processes, e.g., micro IM of heat-sensitive plastics, almost all plastic IM machines are using plasticizing screws. The design and operating principle of such processing machines is described in detail in chapter 1.2.

In particular, the very short cycle times and the use of multiple cavities within an injection mold, make quality control of each manufactured component enormously difficult, which is why the plastics processing industry has usually resorted to line test inspections. In addition, the monitoring of machine values with an initial analysis of their correlation to the crucial quality variables has established itself as a proven method (e.g., [5, 6, 7, 8, 9]). Rapid developments in the field of automation and digitalization of production processes have opened up new opportunities for the IM process to implement the methods created in the context of Industry 4.0 and the Internet of Things (IoT) for linking production chains through communication interfaces. In particular, the Unified Architecture (UA) of the Open Platform Communications (OPC) Foundation standardizes the communication protocol between different machines and peripherals, thus enabling all accruing machine and process data to be collected centrally. Due to the availability of such high-resolution and comprehensive data, machine learning methods can be effectively applied in corresponding production lines. Most of the research in this area is aimed at improving and providing a good prediction of the part quality during the IM process, thereby aiding the machine operator in choosing the optimal machine setpoints (e.g., [10, 11, 12, 13, 14]). A Digital Twin (DT), for example, can represent a combination of the monitoring of process values and the prediction of component quality derived from this. However, its implementation is associated with some challenges, especially in the provision of all machine, process and quality values in sufficient resolution and within the process cycle time.

1.1.1 Digital Twin

A Digital Twin can be defined as a high-fidelity representation of the operational dynamics of its physical counterpart, enabled by near real-time synchronization between the cyberspace and physical space [15]. It can, amongst others, be used for simulation, monitoring and control of the physical asset. Depending on the characteristics of the physical system and also the intended purpose of the Digital Twin, different digital representations are appropriate, i.e., a Digital Twin of a physical system is not a unique entity. A DT intended for monitoring might be significantly different from a DT intended for control of the physical system. The Digital Twin and the Physical Production System (PPS) it represents constitute a Cyber Physical Production System (CPPS). The DT is a prerequisite for developing a CPPS and is also essential for achieving smart manufacturing:

By using a DT in conjunction with optimization procedures the decision-making process of the operator can be aided. Via direct feedback control from the DT to the physical system even autonomous smart manufacturing can be enabled [15]. The benefits for producers are a significant reduction in the manual effort for supervising and controlling CPPSs, which in turn frees up skilled workers.

In companies that use the IM process in series production, one machine operator is usually responsible for monitoring several injection molding machines. This employee usually only intervenes if individual machines indicate a malfunction or if random checks of the manufactured components reveal a quality deviation outside the tolerance limits. Based on experience the machine operator then adjusts the machine setpoints to compensate for the quality deviation. By using DTs of the individual machines, the adjustment of the setting variables is made on the basis of all correlations that influence quality, so that the number of production waste can be significantly reduced by preventing bad part production. In addition, downtimes are reduced and start-up processes are accelerated.

1.1.2 Challenges

Both the realization of a DT and its integration into the CPPS is a challenging task [16]. To mitigate the efforts associated with realizing a DT, reference architectures have been proposed for injection molding [15, 16, 17]. While these works mainly focus on software and data integration, the aspect of how to obtain an accurate Digital Twin, i.e., a dynamical model, of the plastic IM process has not been at the center of attention. As the results of the model-based optimization procedures will heavily depend on the accuracy of the model, this aspect is crucial. In addition, estimating a dynamic model that maps machine and process values to part quality is especially challenging in IM: As opposed to other batch processes, the measurements of part qualities can only be performed at the end of each batch. The DT must therefore be able to map trajectories of machine and process values to a single quantity datum.

A prerequisite for realizing and continuously updating a DT is the measuring of all quantities relevant for predicting part quality. A standard IM machine exclusively measures so-called machine values, i.e., quantities that are measured in the injection molding machine, rather than in the mold cavity where the part is formed. Process values, that describe the state in the cavity, or even quality values, that describe the relevant properties of the produced part and are the ultimate quantity of interest, are not measured. The implementation of the infrastructure (hard- and software-wise) necessary to measure all relevant quantities poses another challenge. Especially the realization of in-line quality measurements, as in-line quality measuring systems are laborious to implement, and some quality variables cannot be measured nondestructively.

Another challenge for quality prediction are external influences that affect the IM process and can have unpredictable effects on the part quality. Due to these influences, the same machine settings at different times can lead to deviating

qualities. Significant influencing factors here are environmental influences, such as temperature and humidity within the production halls, fluctuations within the cooling water circuits, wear of machine and mold components, as well as material-related influences, such as batch fluctuations, varying residual moisture content or deviating mixing ratios. Particularly due to the increased use of recycled materials, the fluctuating material properties have an increasing influence on the part qualities, making a quality prediction very difficult without continuous monitoring of the process variables.

1.1.3 Solution approach

An industrial plastic injection molding machine (ALLROUNDER 470 S, Arburg GmbH + Co KG, Loßburg, Germany), shown in 1.1, is equipped with sensors and an in-line quality measuring system. Thereby all relevant quantities to build a Digital Twin that maps the physical process from machine setpoints $\boldsymbol{s}$ to resulting part quality $\boldsymbol{Q}$ are made available. Different modeling approaches and model structures for obtaining an accurate quality model, which together with the process model constitute the Digital Twin, are investigated and their performances evaluated in a case study. In particular, a novel switched system internal dynamics model approach for building a dynamic quality model is presented. Although not part of this work, the Digital Twin can then be continuously updated via the retrieved machine, process, and quality data. Via model-based numerical optimal control the optimal machine setpoints for a desired quality $\boldsymbol{Q}_{\text{ref}}$ can be calculated from batch to batch, thereby essentially implementing a quality control loop while leaving the machines internal control loops unchanged. The CPPS is depicted in figure 1.2: The given physical assets, i.e., the injection molding machine and the produced part (grey), are augmented via a quality measuring system (green) and via various data interfaces (orange) data is transferred in real-time to the digital twin, i.e., the models and the functions acting on these models (blue).

1.2 PLASTIC INJECTION MOLDING

The basic design of modern injection molding machines is very similar between the different manufacturers and consists of the five functional units that are depicted in figure 1.1. To better understand the impact of the machine parameters and the resulting process values, a typical injection molding cycle as it will be used in the case study will be described before the values itself and the current process control strategies can be explained.

1.2.1 Process cycle and machine components

While the mold specifies the geometry of the component to be produced, the clamping unit performs the mold and ejector movements required during the

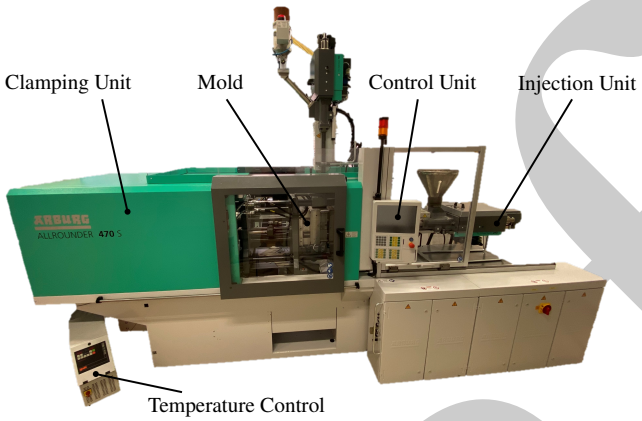

FIGURE 1.1 Injection molding machine ALLROUNDER 470S

injection molding cycle, and provides the clamping force needed to prevent the mold from opening due to high injection pressures. As depicted in Fig. 1.4, the injection unit consists of a hopper, through which the base material is fed into the process in granular form, and a barrel tempered by heating bands, which contains the screw responsible for material conveying, melting and dosing through a rotational movement. In addition, a translatory movement of the screw injects the melted material into the cavity of the mold.

Within the control unit of the machine, the operator can define the process sequence. An exemplary sequence, as also used in the case study, is shown in figure 1.3. First, the mold is closed (1) so that the previously dosed quantity of melt can be injected into the cavity under high pressure (2). To prevent shrinkage of the part during cooling in the mold, a packing pressure is maintained for a defined time after injection (3), allowing the cavity to be kept filled volumetrically. During the subsequent residual cooling time (4), the melt volume required for the next cycle is dosed against a defined back pressure (5) and then relieved by decompression (6). Following the residual cooling time, the mold opens (7) and the ejector movement (8-10) demolds the finished part from the cavity.

1.2.2 Machine setpoints and measured process variables

The production process of an IM machine can be divided into three phases depending on the controlled machine values, i.e., screw velocity and hydraulic pressure. To clarify the screw positions that result from the three phases, they are depicted in figure 1.4.

1) Injection: At the beginning of the injection phase, the screw is in the

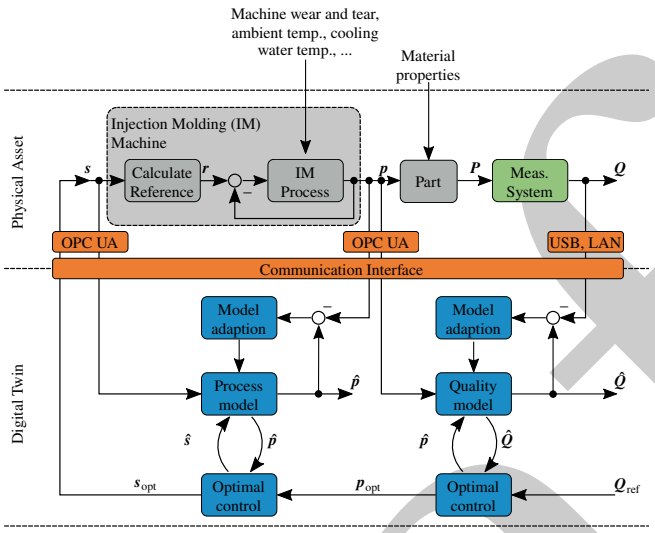

FIGURE 1.2 The devices, models and functions constituting the CPPS of the plastic injection molding process

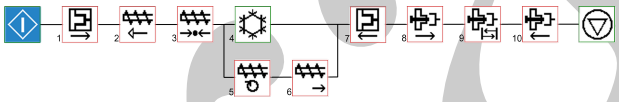

FIGURE 1.3 Injection molding process cycle used in the case study

dosing position. A defined melt volume, located in front of the screw, is then injected at a defined injection velocity until a set switching point is reached, which is defined by the screw position. Since this phase is velocity-controlled, only a hydraulic pressure limit is set on the machine to avoid damage.

2) Packing: To compensate for material shrinkage resulting from cooling, a defined pressure curve over a specified time is needed. Therefore the packing phase is pressure controlled, while the pressure reference signal is composed of multiple consecutive pressure ramps. Three pressure levels were set in the case study presented in this chapter, with only height and duration of the second level being varied as part of the experimental design. The packing phase starts immediately after the screw reaches the switching point and ends after the set time of the pressure levels is over.

3) Cooling: Cooling of the melt begins immediately upon entry into the mold cavity. However, since the time between the start of injection and the end of the packing phase is not sufficient to cool the plastic part to a temperature that assures deformation-free demolding, an additional cooling time is required. Since this cooling phase is pressureless, the injection unit can simultaneously meter the melt volume for the next cycle against a set back pressure so that the

screw is again in the dosing position.

Table 1.1 lists the important machine parameters that were set at the control unit of the IM machine during the case study and the resulting process values that were monitored. The process variables measured in the cavity, i.e., cavity pressure p_{cav} and cavity wall temperature T_{cav}, of a few cycles with different realization of the setpoint $\boldsymbol{s}$ are shown in Fig. 1.5. In addition to the listed variables, for each set target value the corresponding actual values were also recorded. Typically an IM machine records only the trajectories of the clamping and injection unit, i.e., hydraulic pressures, positions and velocities. For monitoring the resulting process values inside the mold cavity, the machine was additionally equipped with a combined pressure and temperature sensor (Type 6190C, Kistler Instrumente GmbH, Sindelfingen, Germany) positioned in the rigid side of the mold. The monitoring and storing of the data will be described in section 1.3.

TABLE 1.1 Machine setpoints $\boldsymbol{s}$ and measured process variables $\boldsymbol{p}(t)$

Machine setpoint s_i	Unit	Process Variable p_i	Unit
Nozzle temperature	°C	Injection pressure	bar*
Mold temperature	°C	Screw position	cm^3
Injection velocity	cm^3/s	Injection velocity	cm^3/s
Switching point	cm^3	Cavity pressure	bar*
Packing pressure	bar*	Cavity wall temperature	°C
Packing time	s		
Back pressure	bar*		
Cooling time	s		

*In IM the pressure is usually measured and stated in bar, therefor no conversion to SI units has been made here.

1.2.3 State of the Art: Process control in injection molding

The injection molding process is affected by various disturbances (e. g. environmental influences, material viscosity, mold temperature, closing behavior, wear and tear of non-return valve) which make a stable production of high-precision components difficult. To compensate these disturbances process control systems are developed. Depending on which variables are controlled, three different control strategies can be distinguished [18]:

- Control of machine values, i.e., process variables that are measured machine-side and therefore reflect the state of the injection molding machine, such as the screw velocity and hydraulic pressure.
- Control of process values, i.e., process variables that are measured cavity-side and therefore reflect the state of the process at the location of part formation, i.e., the cavity. E.g., cavity pressure and temperature.
- Control of quality variables, i.e., the properties of the manufactured parts

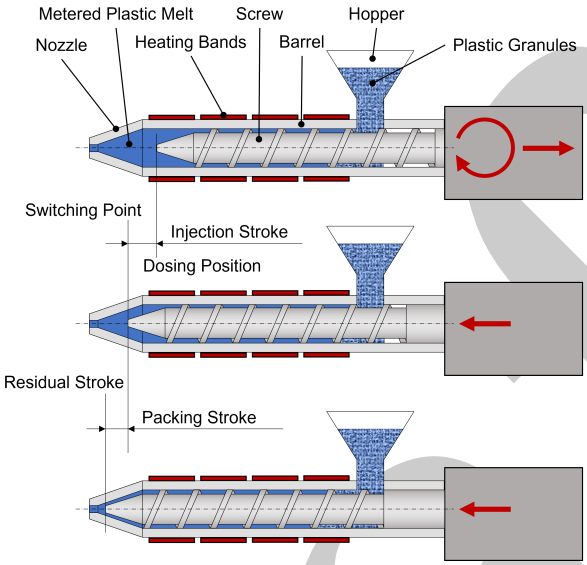

FIGURE 1.4 Schematic illustration of the inside of the injection unit including the movement and important positions of the screw

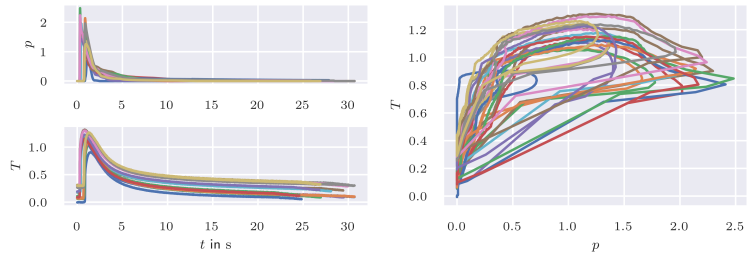

(a) Normalized p_{cav} and T_{cav} signals over time t

(b) Normalized p_{cav} vs. T_{cav}

FIGURE 1.5 Subset of measured normalized cavity pressure p_{cav} and normalized cavity wall temperature T_{cav} signals recorded during execution of the experimental design described in Sec. 1.5.

which contribute to their function

In industrial applications the control of machine values is prevalent. However, aforementioned disturbances affect process values and hence part quality, i.e., part quality may vary even if machine values are reproduced perfectly each cycle [19]. Therefore, the efforts of the scientific community in recent decades have been directed towards the control of in-cavity process-variables, especially the

cavity pressure, which are more closely related to the quality variables. However, due to the nonlinear behavior of the material PID controllers whose parameters are adapted to the current system state are employed for this task. These have to be parameterized for every mold, which is very time-consuming and therefore not suitable for industrial production [19]. To overcome these obstructions to an introduction of cavity pressure control on a wide industrial scale, the concepts of model-based optimization (MO) and iterative learning control (ILC) have been applied [19, 20]: An optimal cavity pressure trajectory is calculated based on the pvT-model (material-specific relationship between pressure p, temperature T and specific volume v), i.e., quality model. Via an ILC, which can be model-free or model-based, the controller output is then adapted from cycle to cycle in order to minimize the tracking error. The control of quality variables has not yet been achieved. The main obstacles being the necessity for in-line quality measurements and a quality model to predict the quality characteristics of the final part.

1.3 DATA ACQUISITION AND MANAGEMENT

In the past, different approaches have been developed for obtaining process data from injection molding processes. Here, too, the approaches differ in the type of data to be obtained. For example, process data describing the behavior inside the cavity of the injection mold can be acquired by additional sensor technology and read out via external monitoring systems [21, 22, 23]. In this way, Ke et al. were able to integrate seven pressure sensors into a mold cavity in order to analyze the filling behavior as precisely as possible [24].

Zhao et al. also used external sensors for process data acquisition, but by doing so they did not record process data in the cavity, but from the injection unit [25]. For this, they used three different types of sensors and data acquisition cards to record pressures, positions, temperatures and times.

To meet the requirements associated with the smart factory concept and Industry 4.0 in terms of communication capability and the degree of interconnectivity along the process chain, machine manufacturers have developed communication interfaces enabling them to integrate their machines into fully networked environments. Most injection molding machines therefore permit not only visualization of the process variables in the machine display, but also provide various export options for the process data generated during the manufacturing process such as USB interfaces [26] or network servers such as the aforementioned Open Platform Communication Unified Architecture (OPC UA) [27].

OPC UA is a platform-independent service-oriented architecture developed by the OPC Foundation as a standard for data exchange between machines and systems. Based on OPC UA, Companion Specifications such as EUROMAP 83 [28] and EUROMAP77 [29] have been developed specifically for plastics processing machines. The Companion Specification EUROMAP77 defines,

among other things, an OPC UA ObjectType that is used for the root object representing an injection molding machine with all its subcomponents. Martins et al. have used this standard to record process parameters such as injection velocity, cycle time and maximum injection pressure [27].

1.3.1 Machine and process values acquisition via OPC UA

Although nearly all machine and process variables can be read out from the injection molding machine via the described standards, this method is only suitable to a limited extent for the formation of Digital Twins, since the data transfer rate is not fast enough for a real-time transfer, especially when several variables are considered. However, in addition to exporting one-time values such as the injection time or the maximum injection pressure, some injection molding machines also allow the export of so-called measurement and monitoring charts (in tabular form) that contain trajectories of set process variables over the cycle time. This can be, for example, the hydraulic pressure or the injection flow trajectories. External sensors that are read out via a measuring amplifier connected to the machine can also be mapped in these charts.

In the case study described in this chapter, a manufacturer-independent python script was developed which exports one-time machine values such as switching point, nozzle and heating band temperatures (including their target and actual values), resulting one-time process variables such as injection time and residual melt volume after the packaging phase, as well as time-series of target and actual process variables such as hydraulic pressure and injection velocity trajectories. Process values such as cavity pressure and temperature time-series were also recorded in this way via the in-mold sensor connected to the injection molding machine.

Within the machine control system, each setpoint and actual value as well as the aforementioned measurement and monitoring charts are assigned an internal manufacturer-dependent label. Via the OPC UA specifications, each of these labels is linked to a unique manufacturer-independent NodeID. The developed script continuously monitors a trigger signal and queries all parameters listed in figure 1.6 after the signal occurs. The trigger signal had to be selected in such a way that, at the time of triggering, all cycle-related process variables relevant for the formation of the Digital Twin were fully mapped in the corresponding charts and the one-time actual values were available. Additionally, after triggering there needs to be enough time to query the values before they were overwritten by the values of the next cycle. Therefore, the opening of the injection mold (7 in figure 1.3) was chosen.

While the monitoring charts only monitor one signal, the measurement charts can include up to four different signals. By dividing the process variables time-series into multiple equally distributed consecutive time-series, that are all mapped in different charts, the frequency of the trajectories can be adjusted. The set recording duration of a chart is thereby divided into 512 equally distributed

```
SIGNALS = {
    'cycle_counter':              signal_struct('ns=2;i=238982'),
    'monitoring_chart_1':         signal_struct('ns=2;i=178052'),
    'monitoring_chart_2':         signal_struct('ns=2;i=179612'),
    'monitoring_chart_3':         signal_struct('ns=2;i=181172'),
    'monitoring_chart_4':         signal_struct('ns=2;i=182732'),
    'monitoring_chart_5':         signal_struct('ns=2;i=184292'),
    'monitoring_chart_6':         signal_struct('ns=2;i=185852'),
    'measurement_chart_1':        signal_struct('ns=2;i=142912', num_signals=4),
    'measurement_chart_2':        signal_struct('ns=2;i=144482', num_signals=4),
    'measurement_chart_3':        signal_struct('ns=2;i=573862', num_signals=4),
    'cycle_time':                 signal_struct('ns=2;i=140842'),
    'heating_zone_1_actual':      signal_struct('ns=2;i=207272'),
    'heating_zone_2_actual':      signal_struct('ns=2;i=207422'),
    'heating_zone_3_actual':      signal_struct('ns=2;i=207572'),
    'heating_zone_4_actual':      signal_struct('ns=2;i=207722'),
    'heating_zone_5_actual':      signal_struct('ns=2;i=207872'),
    'heating_zone_1_target':      signal_struct('ns=2;i=207262'),
    'heating_zone_2_target':      signal_struct('ns=2;i=207412'),
    'heating_zone_3_target':      signal_struct('ns=2;i=207562'),
    'heating_zone_4_target':      signal_struct('ns=2;i=207712'),
    'heating_zone_5_target':      signal_struct('ns=2;i=207862'),
    'injection_velocity_target': signal_struct('ns=2;i=201092'),
    'packing_velocity_1':         signal_struct('ns=2;i=201172'),
    'packing_pressure_1_target': signal_struct('ns=2;i=201292'),
    'packing_velocity_2':         signal_struct('ns=2;i=416782'),
    'packing_pressure_2_target': signal_struct('ns=2;i=201332'),
    'packing_time_2_target':      signal_struct('ns=2;i=201322'),
    'packing_velocity_3':         signal_struct('ns=2;i=416792'),
    'packing_pressure_3_target': signal_struct('ns=2;i=201372'),
    'packing_time_3_target':      signal_struct('ns=2;i=201362'),
    'dosing_volume_target':       signal_struct('ns=2;i=201972'),
    'dosing_volume_actual':       signal_struct('ns=2;i=201732'),
    'switching_point_target':     signal_struct('ns=2;i=201112'),
    'switching_point_actual':     signal_struct('ns=2;i=202422'),
    'residual_volume':            signal_struct('ns=2;i=202672'),
    'backpressure_target':        signal_struct('ns=2;i=201962'),
    'max_pressure':               signal_struct('ns=2;i=202472'),
    'switching_pressure':         signal_struct('ns=2;i=202522'),
    'dosing_time':                signal_struct('ns=2;i=202732'),
    'injection_time':             signal_struct('ns=2;i=202582'),
    'timestamp':                  signal_struct('ns=2;i=117522'),
    }
```

FIGURE 1.6 Recorded charts and values including their corresponding NameSpaceIndex (ns) and NodeID (i)

measuring points due to the programming of the IM machine. By dividing the cycle time over multiple charts, the measuring points add up as a multiple of 512 depending on the number of charts. The maximum frequency at which the sensor values can be recorded is 500 Hz for the machine used. However, since there is only a limited number of available charts (4 measurement charts, 8 monitoring charts and 4 extended monitoring charts), a compromise must be found between achievable frequency and mapping of the relevant time section of the cycle time.

In order to determine an appropriate sampling frequency, the most dynamic signal, i.e., the measured injection pressure, was sampled at the highest sampling rate possible, i.e., 500 Hz. The amplitude and power spectrum are shown in Fig. 1.7. Before applying the Fourier transform the signal was centered and a Hann window was applied to reduce the effect of the offset between the first and last signal value on the spectrum. It can be observed, that the frequencies below 25 Hz account for more than 90 % of the total sum of fourier coefficients and more than 99,9 % of the total signal power. It was therefore concluded that a sampling rate of 50 Hz is sufficient for data acquisition. To achieve this sampling rate in the case study, the cycle time had to be divided among three consecutive charts, each with a recording duration of 10.16 s. The process variables were divided among the various charts as follows:

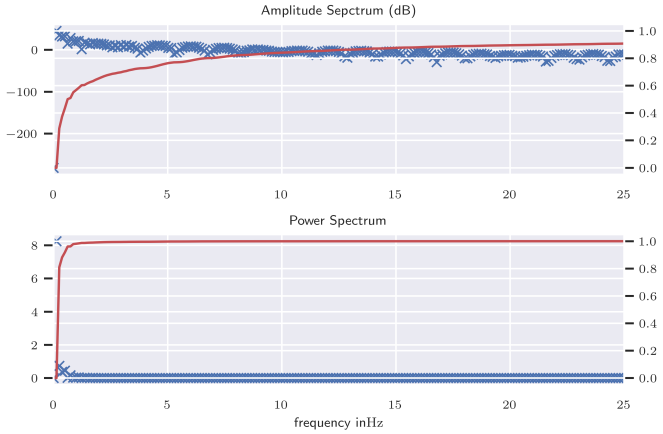

FIGURE 1.7 First part of amplitude Spectrum (above) and power spectrum (below) of the injection pressure signal sampled at 500 Hz. The red curve represents the share of cumulative sum up to the respective frequency relative to the total sum.

- Monitoring charts 1-3: injection velocity
- Monitoring charts 4-6: screw position
- Measurement charts 1-3: target and actual injection pressure, pressure and temperature in the mold cavity

The segmentation of the cycle time among the three charts is depicted in Fig. 1.8. The recording of the displayed trace starts directly at the beginning of the process cycle and ends when the trigger is reached. In the case study this trigger was chosen to be the opening of the injection mold (7 in Fig. 1.3). Data during the time span Δt, which occurs between the trigger and the start of the next cycle, is not recorded, as it is not relevant for model building. Within this time span only the injection mold moves, which is not relevant for part quality.

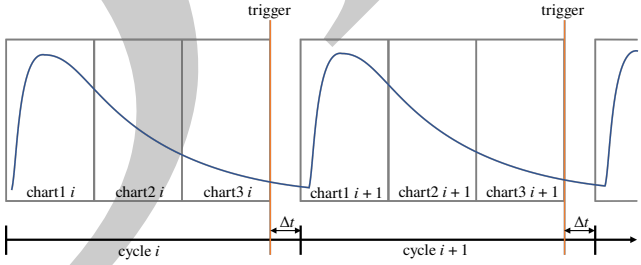

FIGURE 1.8 Visualization of splitting each cycle time into three charts.

All recorded machine and process variables are stored in a Hierarchical

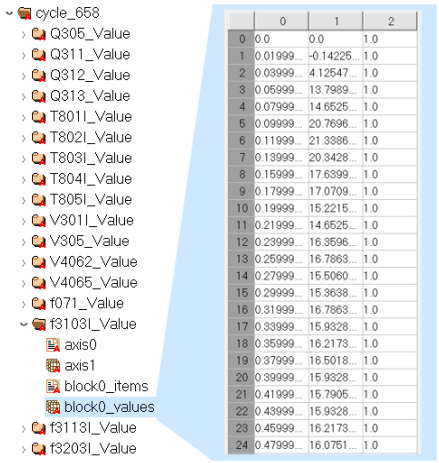

FIGURE 1.9 Structure of the HDF5 file

Data Format 5 File (HDF5) in a cycle-related manner. Figure 1.9 shows the chosen structure of the files. For simplified visualization, each parameter is denoted with the manufacturer-dependent label and unambiguously assigned to the corresponding cycle. For each parameter, the corresponding recorded value (block0_values) is stored in addition to the description (block0_items) shown in figure 1.6. The charts, e.g., f3103I, are stored in tabular form, as shown in figure 1.9, where column 0 represents the time, 1 the value of the injection velocity at the corresponding time and 2 the machine state (not considered in this study).

1.3.2 In-line part quality data acquisition

In IM series production with very short cycle times and, possibly, multi-cavity injection molds, in-line quality control is very costly and in some cases the costs exceed the benefits. However, especially in the case of complex technical components, which are subject to high requirements in terms of load-bearing capacity, durability and optical properties, undetected quality deviations can result in costly consequences. Quality control of every manufactured part is desirable, but it is not possible to record all relevant quality characteristics within the process cycle and to measure non-destructively. Quality parameters that can be detected in the process cycle include weight and geometric tolerances such as dimensions, shrinkage and warpage, but also optically detectable defects such as sink marks, color differences, streaks and weld lines. Since quantifiable values are recorded by measuring the component weight and its dimensions, and conclusions can be drawn about the process behavior with the aid of these quality variables, these characteristics were taken into account in the case study. For this purpose, both a scale (Entris II, Sartorius AG, Göttingen, Germany) and

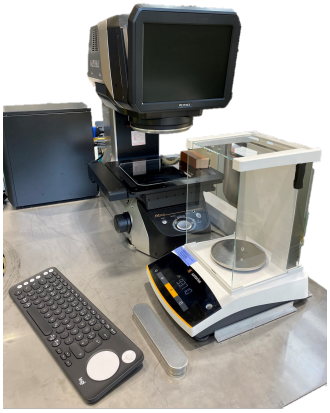

FIGURE 1.10 Quality measuring setup including a scale to measure the parts weight and a digital measurement projector to measure the parts dimensions

a digital measurement projector (IM-7020, Keyence Corporation, Osaka, Japan) were integrated into the process (Fig. 1.10). These measurements are carried out manually. Since the quality variables are recorded within the process cycle time by this measurement setup, they can be assigned to the cycle-based process data. However, the quality characteristics of the part produced in cycle i can only be measured during cycle $i + 1$ (Fig. 1.8).

Fig. 1.11 shows the tamper-evident closure, that was produced in the case study and its dimensions, are measured with the measurement projector. While only the diameter of the perforated circle [1], that will be denoted as inner diameter D_i in the case study, was measured on the upper side of the closure, both the diameter [2] and the roundness [5] were determined for the outer diameter on the lower side. As further quality characteristics, the web widths [3] and [4] were measured on both sides of the perforated circle.

1.4 CONTROL-ORIENTED MODELING OF FINAL-PART QUALITY

A data-driven internal dynamics approach for dynamic modeling of the quality characteristics is developed. The proposed approach is in principal a nonlinear state-space model capable of mapping process value trajectories to final part quality. This quality model can be employed to calculate reference process value trajectories via numerical optimal control. In contrast to pvT-optimization (section 1.2.3) the data-driven quality model does not rely on any assumptions and is able to map arbitrary process values to part quality. This means in turn that based on this model not only reference trajectories for cavity pressure, but for all process variables deemed relevant can be generated. Also, the process values trajectories are optimized directly with respect to part quality as opposed

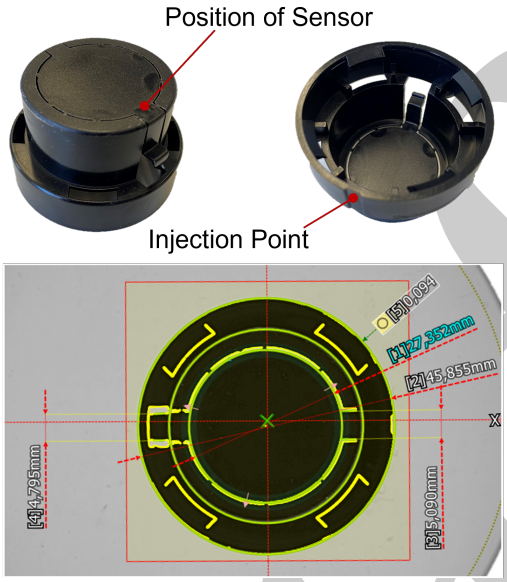

FIGURE 1.11 Tamper-evident closure and its geometrical dimensions (screenshot from measuring projector) measured in the case study ([1] inner diameter D_i, [2] outer diameter D_o, [3] width at joint W_j, [4] width at tab W_t, [5] roundness ○).

to minimal shrinkage, as is the case in pvT-optimization. The downsides of the proposed approach are that the resulting parameter estimation problem is rather complex and time-intensive to solve and the well known need of most data-driven approaches for a rather substantial amount of data for training.

1.4.1 Final part quality prediction

In order to obtain a consistent and desirable batch end-product quality, precise quality prediction models are necessary that can be employed for in-batch or batch-to-batch optimization. Many batch processes, such as the plastic injection molding process, do not allow for continuous in-process quality measurements. Quality variables of interest, e.g., weight, density or geometrical features, can only be quantified once the part is ejected from the machine. The task of predicting the quality characteristics of the emerging part at the end of the batch is known as final part quality prediction [30]. Although the formation of quality characteristics is a dynamic process, i.e., its future evolution is a function of its current state, it has almost exclusively been treated as a static modeling task [31, 32, 13, 24, 33, 30]. One of the reasons is, that the estimation of a dynamic model that maps process value trajectories to a single batch-end quality measurement is an unusual and difficult modeling task.In plastic injection molding final part quality is usually directly predicted from process setpoints [32,

16]. This approach works reasonably well, as long as the process is operating at steady-state, process dynamics do not change and no disturbances act on the process. In plastic injection molding processes with cavity pressure control, the cavity pressure reference trajectory can be derived from the pvT-diagram of the material. This is known as pvT optimization [34]. The pressure reference trajectory is derived from the pvT-diagram with the intent to obtain a part with a certain specific volume v and minimize shrinkage in the process. pvT-optimization does not provide a link to any other quantity that may be of interest, such as surface characteristics or mechanical properties of the produced part. In particular Hopmann et al. [23] documented, that in an injection compression molding application, the cavity pressure trajectory that yielded the best quality differed from the pressure trajectory that led to the least shrinkage. This suggests that apart from cavity pressure other process values have to be taken into account and that minimizing shrinkage does not ensure optimal part quality in every regard.

In most applications beside plastic injection molding multivariate statistical process control (MSPC) methods, such as multi-way principal component analysis (MWPCA) and multi-way projection to latent structures (MWPLS), are employed to correlate process variable trajectories with final product quality [35]. Although these methods exploit all the information in the data, as static models they are subject to certain restrictions, e.g., that all batches need to have the exactly same duration [33]. Hence, methods must be employed that somehow scale all trajectories to the same length, e.g., Dynamic Time Warping. By doing so, the original information contained in the measured data is affected to an unknown extent.

1.4.2 Preliminaries

Dynamic models can amongst other criteria be differentiated into *external* and *internal dynamics* approaches, see Fig. 1.12. In the far more widespread external dynamics approach a static model $\boldsymbol{f}(\cdot)$ is provided with past inputs $\boldsymbol{u}_{k-j} \in \mathbb{R}^{n_\mathrm{u}}$ $j = 1, \ldots, n$ and outputs $\boldsymbol{y}_{k-i} \in \mathbb{R}^{n_\mathrm{y}}$ $i = 1, \ldots, m$ to predict the current output $\boldsymbol{y}_k$. I.e., the dynamics are realized via external filters that in their most simple form correspond to time-delays. The model equation for a time-invariant external dynamics model without dead time is:

$$\boldsymbol{y}_k = \boldsymbol{f}\left(\boldsymbol{y}_{k-1}, \ldots, \boldsymbol{y}_{k-m}, \boldsymbol{u}_{k-1}, \ldots, \boldsymbol{u}_{k-n}\right) \tag{1.1}$$

In (1.1) q^{-1} is the time-shift operator, i.e., $q^{-1}\boldsymbol{u}_k = \boldsymbol{u}_{k-1}$. The internal dynamics approach realizes process dynamics not via external filters, but via internal model states $\boldsymbol{x}_k \in \mathbb{R}^{n_\mathrm{x}}$ and therefore results in a state space representation of the identified system. The states do usually not have any physical meaning and are merely a means of realizing dynamic behavior. An internal dynamics model is

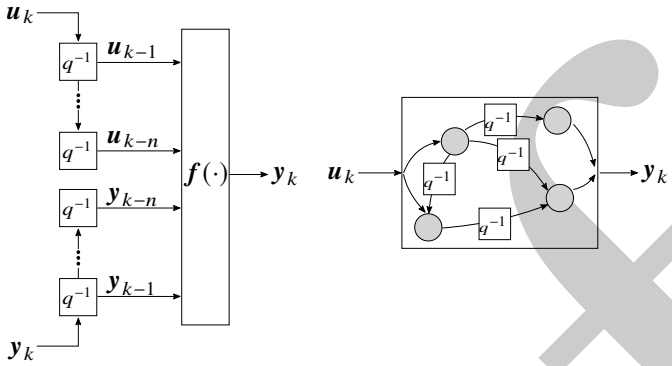

FIGURE 1.12 External (left) and internal dynamics approach (right)

provided with the current input and the previous state to predict the next output:

$$\begin{aligned} \boldsymbol{x}_{k+1} &= \boldsymbol{h}\left(\boldsymbol{x}_k, \boldsymbol{u}_k\right) \\ \boldsymbol{y}_k &= \boldsymbol{g}\left(\boldsymbol{x}_k\right) \end{aligned} \tag{1.2}$$

Both the external and internal dynamics approaches are viable for the problem of final part quality prediction from process value measurements. Irrespectively of the chosen dynamics, models can only be trained in *parallel* configuration, i.e., as simulation or output-error (OE) model. Training in *series-parallel* configuration, i.e., as one-step ahead predictor or equation-error model, is not possible since the model output $\hat{\boldsymbol{y}}_k$ is only available at the very last time instance $k = T$ of each batch. This also means, that only the prediction error of the last time step $\boldsymbol{e}_T = \hat{\boldsymbol{y}}_T - \boldsymbol{y}_T$ is available for calculating the parameter updates during optimization, i.e., in case of a quadratic loss function:

$$\mathcal{L} = \frac{1}{2}\left(\hat{\boldsymbol{y}}_T - \boldsymbol{y}_T\right)^T \left(\hat{\boldsymbol{y}}_T - \boldsymbol{y}_T\right) \tag{1.3}$$

Major advantages of the internal dynamics approach are the lower dimensional input space especially for higher order multiple-input and multiple-output (MIMO) systems and that most advanced controller synthesis methods require a state-space representation. Additionally, determining the dynamic order can be cumbersome in case of an external dynamics approach, especially in the multiple-input and multiple-output (MIMO) case and if input and output are allowed to have different delays. In an internal dynamics approach determining the order of the models equates to choosing the dimension of the internal state vector. However, training recurrent model structures poses a complex optimization problem: The evolution of the internal states must reflect the true process dynamics, but can only be deduced from input-output data. In the external dynamics approach on the other hand, the process dynamics are fixed by the filters specified by the user.

In the last decade, recurrent model structures that alleviate these problems have been developed. Most notably the long short-term memory (LSTM) [36] and the gated recurrent unit (GRU), which will both be subsumed under the term Gated Units in the following. Although a subject of ongoing research, it appears that Gated Units restrict the dynamics that can be represented in comparison to traditional Recurrent Neural Network approaches. This results in fewer bifurcation boundaries and hence fewer regions with very large gradients in the model parameter space, which makes them less sensitive to initialization and easier to train [37]. In the following, modeling approaches for predicting final part quality with external and internal dynamics models will be presented. External dynamics models without output feedback, e.g., Finite Impulse Response (FIR) and its nonlinear variants, will be excluded from consideration. These models treat each time instance as a distinct input. This would result in thousands of inputs (and model parameters) depending on the length and number of measured process variables. The amount of experimental data needed to estimate these parameters makes this approach unfeasible.

1.4.3 Internal dynamics quality model

The machine-value-controlled PIM process is a time-varying process due to the switching between different controllers at defined switching time instances between the injection, packing and cooling phases. The formation of the part's quality characteristics can also be assumed to be a time-varying process, although for different reasons: The part changes its aggregate state from fluid to solid and hence its mechanical properties. A fluid will respond differently, e.g., to a certain applied pressure, than a solid body. Accounting for this time-varying behavior could be done by assuming the model parameters are functions of the internal model states, but this would further exacerbate the complexity of the optimization problem. The quality model was therefore assumed to be a time-varying switched system comprised of three time-invariant subsystems, respectively representing the injection, packing and cooling phase $i = 1, 2, 3$. The parameter vectors of the state equation and output equation of each subsystem are denoted $\boldsymbol{\Theta}^i$ and $\boldsymbol{\Phi}^i$ respectively.

$$\begin{aligned} \boldsymbol{x}_{k+1} &= \boldsymbol{h}^i\left(\boldsymbol{x}_k, \boldsymbol{u}_k; \boldsymbol{\Theta}^i\right), \quad \boldsymbol{x}_0 = \boldsymbol{0}, \quad k \in \mathbb{Z}, \quad i = \begin{cases} 1 \;\forall\; k \leq t_1, \\ 2 \;\forall\; t_1 < k \leq t_2, \\ 3 \;\forall\; k > t_2 \end{cases} \\ \boldsymbol{y}_k &= \boldsymbol{g}^i\left(\boldsymbol{x}_k; \boldsymbol{\Phi}^i\right) \end{aligned} \tag{1.4}$$

The switching time instances t_i coincide with the end of the respective phase and are known in advance. Since the internal state is thought to be an, albeit very abstract, representation of the emerging part, the model is assumed to be continuous in the states. I.e., all subsystems are of the same order and at the switching instances $\boldsymbol{x}_{t_i}^{i+1} = \boldsymbol{x}_{t_i}^{i}$ holds. The unfolded switched system is depicted

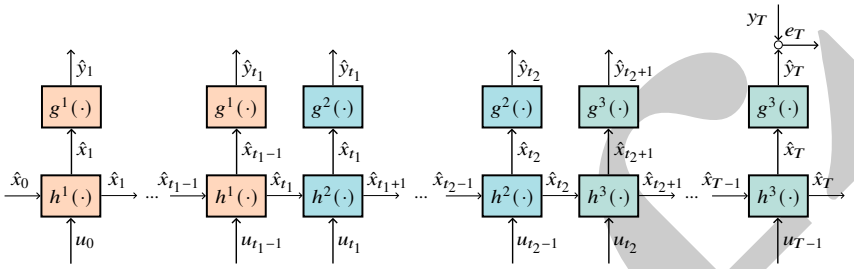

FIGURE 1.13 Switched internal dynamics model for final part quality prediction

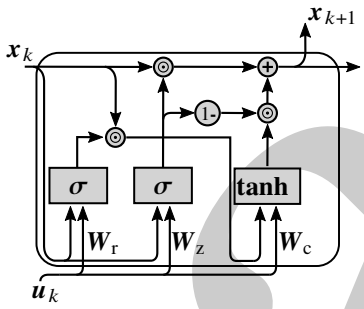

FIGURE 1.14 Gated Recurrent Unit architecture

in Fig. 1.13. For the aforementioned reasons, the recurrent part $\boldsymbol{h}^i(\cdot)$ of each subsystem will be modeled using a Gated Recurrent Unit. The GRU is depicted in Fig. 1.14. Its state equation is:

$$\boldsymbol{x}_{k+1} = \boldsymbol{f}_z \odot \boldsymbol{x}_k + (\mathbf{1} - \boldsymbol{f}_z) \odot \boldsymbol{f}_c. \tag{1.5}$$

The operator $\odot$ denotes the Hadamard product. The activation of the so-called reset gate $\boldsymbol{f}_r$, update gate $\boldsymbol{f}_z$ and the output gate $\boldsymbol{f}_c$ is given by

$$\begin{aligned} \boldsymbol{f}_r &= \boldsymbol{\sigma}\left(\boldsymbol{W}_r \cdot [\boldsymbol{x}_k, \boldsymbol{u}_k]^T + \boldsymbol{b}_r\right), \\ \boldsymbol{f}_z &= \boldsymbol{\sigma}\left(\boldsymbol{W}_z \cdot [\boldsymbol{x}_k, \boldsymbol{u}_k]^T + \boldsymbol{b}_z\right), \\ \boldsymbol{f}_c &= \mathbf{tanh}\left(\boldsymbol{W}_c \cdot [\tilde{\boldsymbol{x}}_k, \boldsymbol{u}_k]^T + \boldsymbol{b}_c\right), \end{aligned} \tag{1.6}$$

with $\tilde{\boldsymbol{x}}_k = \boldsymbol{f}_r \odot \boldsymbol{x}_k$ and $\boldsymbol{W}_r, \boldsymbol{W}_z, \boldsymbol{W}_c \in \mathbb{R}^{n_x \times n_x + n_u}$, $\boldsymbol{b}_r, \boldsymbol{b}_z, \boldsymbol{b}_c \in \mathbb{R}^{n_x}$ and $\boldsymbol{f}_r, \boldsymbol{f}_z, \boldsymbol{f}_c : \mathbb{R}^{n_x} \to \mathbb{R}^{n_x}$. $\boldsymbol{\sigma}(\cdot)$ denotes the logistic function and $\mathbf{tanh}(\cdot)$ the hyperbolic tangent function. Both are applied element-wise.

The feedforward-part $\boldsymbol{g}^i(\cdot)$ continuously maps the internal model state $\boldsymbol{x}_k$ to the model output $\boldsymbol{y}_k$. However, only $\boldsymbol{y}_T$, i.e., the part quality measurement at the very last time instance T of each batch, is measured. Therefore $\boldsymbol{\Phi}^i$, $i = 1, 2$, will not enter the loss function as it has no effect on $\boldsymbol{y}_T$ and will not be adjusted

during training. Usually, a feed forward Neural Network with a nonlinear hidden layer and a linear output layer is employed:

$$\begin{aligned} \boldsymbol{h}_k &= \mathbf{tanh}\left(\boldsymbol{W}_\mathrm{h} \cdot \boldsymbol{x}_k + \boldsymbol{b}_\mathrm{h}\right) \\ \boldsymbol{y}_k &= \boldsymbol{W}_\mathrm{o} \cdot \boldsymbol{h}_k + \boldsymbol{b}_\mathrm{o} \end{aligned} \tag{1.7}$$

$\boldsymbol{h}_k$ is the activation of the neurons in the hidden layer. Parameter initialization was found to be crucial in order to obtain useful models. As in any (stable) dynamical system the contribution of the GRU's state $\boldsymbol{x}_k$ at a given time instance k to the output $\boldsymbol{y}_{k+\Delta T}$ at a later time instance decreases exponentially with ΔT. Since the model to be optimized is recurrent in the states, the same is true for its parameters. This phenomenon is known as the *vanishing gradient* problem. If care is not taken during initialization, especially the contribution of the first two subsystems ($i = 1, 2$) will be negligible small. The solution to this dilemma is to initialize the bias of the update gate $\boldsymbol{b}_\mathrm{z}^i$ $i = 1, 2$ with large positive values. By doing so the state equation (1.5) becomes $\boldsymbol{x}_{k+1} \approx \boldsymbol{x}_k$, i.e., the GRU just passes on the state. This ensures the maximal possible gradient, at least at the very beginning of the optimization procedure. If need be, the optimizer will then reduce the bias to an appropriate value, such that the GRU's dynamics approximates the dynamics of the true process. For this reason the bias must also not be chosen too large, otherwise it would take an excessive amount of optimization steps to reduce it to an appropriate value. For this case study, the best results were obtained by drawing $\boldsymbol{b}_\mathrm{z}$ from a random uniform distribution $\mathcal{U}_{[4,10]}$. Without this initialization the estimated models were merely able to reproduce the mean of the training data.

1.4.4 External dynamics quality model

Although no continuous output measurements are available, the external dynamics approach is still applicable: The model is trained in parallel configuration, i.e., as a simulation model, i.e., output measurements are not required when evaluating the model. It should be noted, that a recommended initialization strategy for output-error (OE) models is to train the model as a one-step-âhead predictor and use the result to intialize the OE optimization. This procedure can potentially yield an initial parameterization that is close to a good local minimum of the NOE loss function. Due to lacking continuous output measurements this procedure cannot be applied and one has to resort to random initialization. As discussed in section 1.4.3 a switched system approach with three subsystems is chosen to model the time dependency of the formation process of the part's quality characteristics. For convenience of notation the maximum time delay of the input and output are assumed to be equal and each subsystem is assumed to

have the same maximal delay n:

$$\hat{\boldsymbol{y}}_k = \boldsymbol{f}^i\left(\begin{bmatrix}\hat{\boldsymbol{y}}_{k-1} & \dots & \hat{\boldsymbol{y}}_{k-n} & \boldsymbol{u}_{k-1} & \dots & \boldsymbol{u}_{k-n}\end{bmatrix}^T;\boldsymbol{\theta}^i\right)$$
$$\hat{\boldsymbol{y}}_i = \boldsymbol{0}\ \forall\ j = 1,\dots,n-1 \qquad k \in \mathbb{Z}, \quad j = \begin{cases}1\ \forall\ k \le t_1,\\ 2\ \forall\ t_1 < k \le t_2,\\ 3\ \forall\ k > t_2\end{cases} \tag{1.8}$$

Since the external dynamics approach requires the (unknown) first n output measurements as initialization, they are set to zero in accordance to the internal dynamics model (1.4). The unfolded external dynamics switched system is depicted in Fig. 1.15. As the external model is to be trained in parallel con-

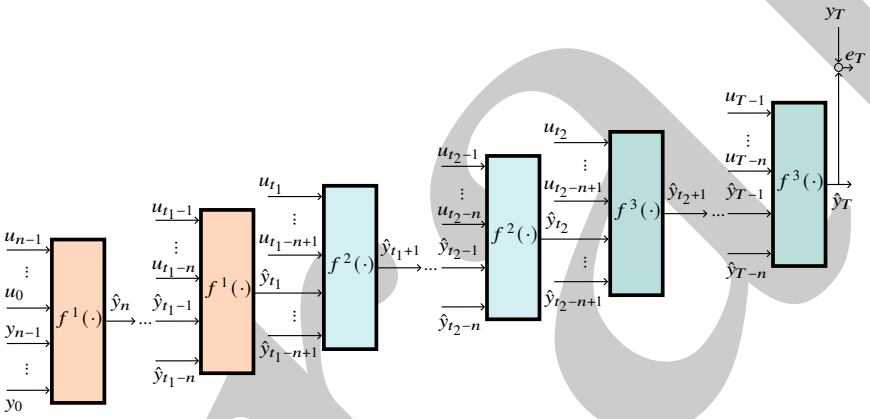

FIGURE 1.15 Switched external dynamics model for final part quality prediction

figuration, care has to be taken that the initial model is not unstable. Finding a stable parameterization for a nonlinear model is difficult. It is easier to choose a model structure whose output cannot blow-up by design. A multilayer perceptron (MLP) with bounded activation functions satisfies this assumption, as opposed to a polynomial model e.g., and is therefore an appropriate candidate structure.

1.4.5 Static quality model

Estimating a static model that maps process setpoints, i.e., $\boldsymbol{u} = \boldsymbol{s}$, to final part quality, i.e., $\boldsymbol{y} = \boldsymbol{Q}$, can be considered as the current industrial state-of-the-art. This approach will therefore be considered as baseline in the subsequently presented case study. Employing a static model entails the implicite assumption that the process is at steady state. This implies that data collected for a number of cycles after changing the process setpoint cannot be used for model estimation, increasing the time spent on collecting data for model training. In addition,

during process operation the model cannot be used whenever even minor disturbances occur, such as variations in the time interval between cycles, e.g., because a part got stuck. As these events happen quite frequently, it is proposed to include process value measurements at the beginning of a cycle, i.e., $\boldsymbol{p}_0 = \boldsymbol{p}(t = 0)$ as inputs to the static model, i.e., $\boldsymbol{u}^T = \left[\boldsymbol{s}^T, \boldsymbol{p}_0^T\right]$. By doing so, the initial state of the process is explicitely considered. A variations in the time between cycles would become visible in different temperatures of the mold cavity. The model equation of the static approach is simply

$$\boldsymbol{y} = \boldsymbol{f}(\boldsymbol{u})$$

1.5 CASE STUDY: TAMPER-EVIDENT CLOSURE QUALITY PREDICTION

To investigate whether dynamic quality models have additional value compared to the less complex and less time-consuming static approach, a case study is conducted. The objective of this case study is the prediction of the mass m and inner diameter D_i of the tamper-evident closure depicted in Fig. 1.11. The material chosen for the production of this closure is an unreinforced black polyamide 6 (PA6) of the type B3S (BASF SE, Ludwigshafen am Rhein, Germany).

In order to effectively train models, the training data must originate from as large a process window as possible, to include all correlations and non-linear effects of the processing parameters. However, a compromise must be found between a large process window, the achievable quality and the processability of the material. A large number of Design of Experiments (DoE) have been developed to analyze precisely such correlations between the individual parameters and to describe them by means of regression analyses. Since the injection molding process reacts very sluggishly when certain parameters are varied (e.g., temperatures) and it takes several cycles until a constant process is established again after the change, randomized experimental designs, such as Latin Hypercubes, are sometimes difficult to implement in the real process. Heinisch et al. compared the performance of artificial neural networks trained with data retrieved from different DoEs used in IM simulations [38]. It could be shown, that central composite designs (CCD) outperformed the other DoEs and thus provide the best data basis for training neural networks. CCDs extend a full factorial design (FFD) by so-called star points (SP) that are located exactly on the coordinate axes and have a distance α to the origin, which is the central point (CP) of the FFD. For this case study a process setpoint $\boldsymbol{s} \in \mathbb{R}^8$ is defined by the eight setpoint parameters defined in Tbl. 1.2. With two factor levels for each setpoint parameter and two repetitions of the central point (for the estimation of process dispersion), the resulting experimental design contains a total of 274 experiments (FFD: $2^8 = 256$, SP: $2 \cdot 8 = 16$, CP: 2) with 10 repetitions each. A face centered CCD ($\boldsymbol{\alpha} = 1$) was chosen.

TABLE 1.2 Upper and lower limits of the setpoint parameters used for the face centered composite design of experiment.

Setpoint Parameter	Unit	Lower limit	Upper limit
Nozzle temperature	°C	250	260
Mold temperature	°C	40	50
Injection velocity	cm^3/s	16	48
Switching point	cm^3	13	14
Packing pressure	bar*	500	600
Packing time	s	3	5
Back pressure	bar*	25	75
Cooling time	s	15	20

*In IM the pressure is usually measured and stated in bar, therefor no conversion to SI units has been made here.

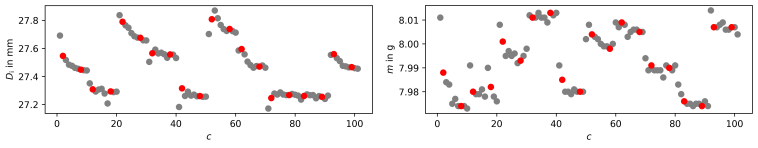

(a) D_i **(b)** m

FIGURE 1.16 Measured inner diameter D_i and mass m of the tamper-evident closure over the first ten charges. Grey samples were used for training, red samples for model validation.

For the production of the parts the aforementioned IM machine (Fig. 1.1) was used. The injection mold was equipped with an additional combined temperature and pressure sensor, as described in 1.2.2. During the manufacturing of the parts only the setpoins listed in Tbl. 1.2 were varied according to the face centered CCD and for each experiment ten parts were produced.

A subset of the acquired data, i.e., the first ten factor combinations, are depicted in Fig. 1.16. From Fig. 1.16 it can be observed, that the process setpoint has a noticeable effect on the parts inner diameter D_i and mass m.

It can also be observed, that different process setpoints also lead to distinctively different process variable trajectories. Fig. 1.17 i shows the cavity-pressure p_{cav} and cavity-temperature T_{cav} of different factor combinations that respectively corresponded to a part with small, medium or large inner diameter D_i. It is also evident from Fig. 1.16 that with respect to the quality variables a good amount of variation also exists within most factor combinations. Especially the with respect D_i a pronounced transient behavior is noticable. In order for a dynamic quality model to predict these variations, they must be reflected in the process measurements. Therefore, the cavity-pressure p_{cav} and cavity-temperature T_{cav} of factor combinations with and without pronounced transient behavior with respect to D_i were investigated. As an example, the measurements of the first

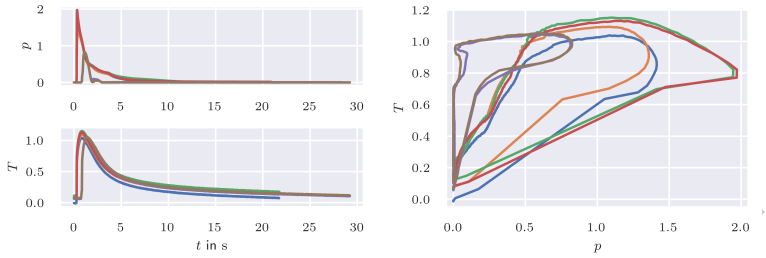

(a) Cavity pressure $p(t)$ and temperature $T(t)$ over time t

(b) $p(t)$ vs. $T(t)$

FIGURE 1.17 Process measurements from three different factor combinations (cycles 1-10,51-61 and 71-81)

(cycles 1-10) and ninth factor combination (cycles 81-90) are shown in Fig. 1.18 and 1.19 respectively. The process measurements taken during the cycles of the first factor combination are appreciably different from another, while there is barely any difference between the process measurements of the ninth factor combination. Most noticeable is a significant increase in the initial and maximal cavity temperature T_{cav} over the first ten cycles, which isn't the case during cycles 81 to 90. This effect is due to the fact, that some setpoint changes require more time than others, which allows the mold more or less cool-down time. In addition, the cavity pressure trajectories vary most around $t \approx 2.5$ s. Closer inspection revealed that the cause was an increase in cavity pressure, that took place at different points at time, but precisely when the measured cavity pressure was 104 °C. Most likely the pressure spike was due to changes on the level of the microstructure which occured at different points in time as a result of different initial cavity temperatures. Based on these observations, the cavity temperature is expected to be a decisive quantity in predicting part quality.

Of each factor combination the second and the third last repetition were chosen as validation data $\mathcal{D}_{\text{val}}$, while the remaining data $\mathcal{D}_{\text{train}}$ was used to train the model. By doing so it was made sure that the models ability to explain the transient behavior is validated. The model structures considered for this task are listed in Tbl. 1.3. Implementation and optimization of all nonlinear models was performed using Casadi [39] and Ipopt [40]. 20 multi-starts were performed for each candidate structure. The performance of each model configuration is measured in terms of the Best Fit Rate (BFR), which corresponds to the coefficient of determination restricted to positive values:

$$\text{BFR} = \max\left(0, 1 - \frac{\sum_c y_c - \hat{y}_c}{\sum_c y_c - \bar{y}_c}\right) \tag{1.9}$$

The performance in terms of the best fit rate (BFR) (1.9) on $\mathcal{D}_{\text{val}}$ of each model

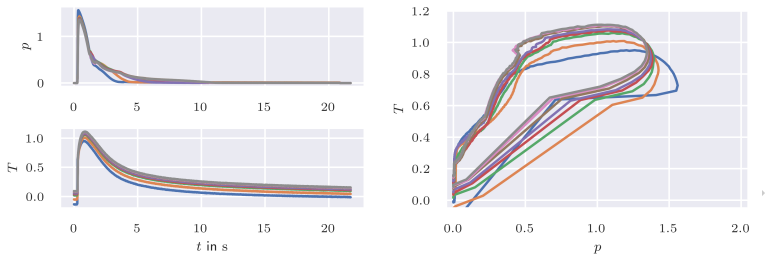

(a) Cavity pressure $p(t)$ and temperature $T(t)$ over time t

(b) $p(t)$ vs. $T(t)$

FIGURE 1.18 Process measurements from factor combinations cycle 1-10

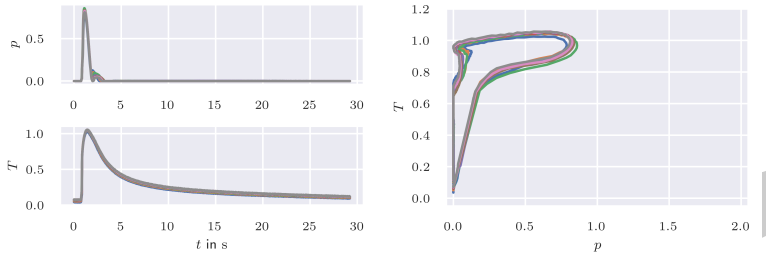

(a) Cavity pressure $p(t)$ and temperature $T(t)$ over time t

(b) $p(t)$ vs. $T(t)$

FIGURE 1.19 Process measurements from factor combinations cycle 71-81

TABLE 1.3 Considered candidate model structures for quality prediction.

Label	Dynamics	Definition
$\mathrm{PR}_{\mathrm{s}}^{n}$	static	n-th degree polynomial regression (PR) model with interactions mapping process setpoints $\boldsymbol{s}$ and possibly initial process value measurements $\boldsymbol{p}_0$ to product quality $\boldsymbol{Q}$.
$\mathrm{MLP}_{\mathrm{s}}^{n}$	static	MLP with n neurons in single hidden layer mapping process setpoints $\boldsymbol{s}$ and possibly initial process value measurements $\boldsymbol{p}_0$ to product quality $\boldsymbol{Q}$.
ED^{n}	ext. dynamics	External dynamics (ED) model consisting of 3 subsystems mapping process measurements $\boldsymbol{p}$ to product quality $\boldsymbol{Q}$, as described in Sec. 1.4.4
ID^{n}	int. dynamics	Internal dynamics (ID) model consisting of 3 subsystems mapping process measurements $\boldsymbol{p}$ to product quality $\boldsymbol{Q}$. The recurrent model part is realized via GRUs with n internal states. The mapping from internal state to product quality is realized via an MLP with 10 $\tanh$ neurons in the hidden layer.

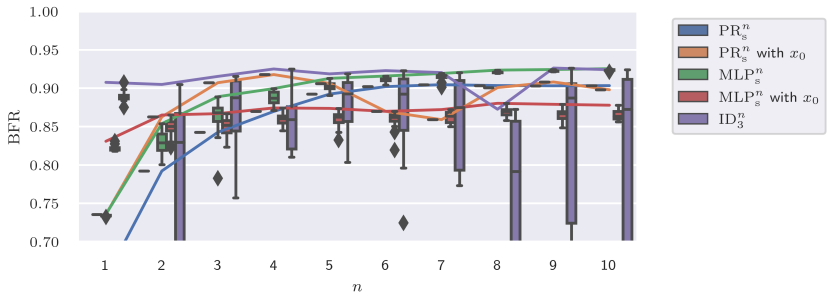

FIGURE 1.20 BFR of the model structures in Tbl. 1.3 on the quality prediction task tamper evident closure.

structure is depicted in Fig. 1.20. For model structures that are nonlinear in the parameters a boxplot is given to visualize the effect of initialization dependence. The lines connect the best identified model respectively. The first thing standing out from Fig. 1.20, is that the proposed switched internal dynamics approach ID consistently yields the model with the best fit, with the exception of $n = 9$ internal states. For this configuration the optimizer was apparently not able to find a good local optimum. The superior performance of the internal dynamics models is remarkable, since the task of predicting batch end quality from raw sensor measurements is considerably harder than a static mapping from setpoints to part quality. The results regarding the polynomial models PR and the MLP seem somewhat conflicting. Comparing the polynomials models with and without initial process measurements x_0 suggests, that the additional information helps predicting part quality, as PR_s^4 with x_0 is the best polynomial model. The decreasing performance for PR_s^n with x_0 for $n > 4$ is most likely due to the tendency of higher degree polynomials for oscillatory interpolation behavior. The best MLP and second best model overall on the other hand is $\mathrm{MLP}_\mathrm{s}^{10}$, a purely static MLP, which does not receive initial process measurements x_0 as input. As discussed previously, variations in quality measurements are larger between factor combinations than within a factor combination and are therefore mostly governed by the machine setpoint. A good fit of the static model was therefore expected. It is however surprising, that the MLPs without initial process measurements x_0 performed as well as the internal dynamics model in terms of the Best Fit Rate. To investigate this outcome, the predictions of the best internal dynamic model, ID_3^4, the best static model with initial process measurements PR_s^4 with x_0, and the best static model without initial conditions, $\mathrm{MLP}_\mathrm{s}^{10}$, on $\mathcal{D}_\mathrm{train}$ and $\mathcal{D}_\mathrm{val}$ are compared, see Fig. 1.21. Fig. 1.21 shows that the models using process measurements to predict part quality are able to explain variations within the same setpoint (factor combination) reasonably well. The reason why $\mathrm{MLP}_\mathrm{s}^{10}$ has a slightly higher BFR than PR_s^4 with x_0 despite not being able to explain any variation within a certain setpoint becomes apparent from the histograms of the

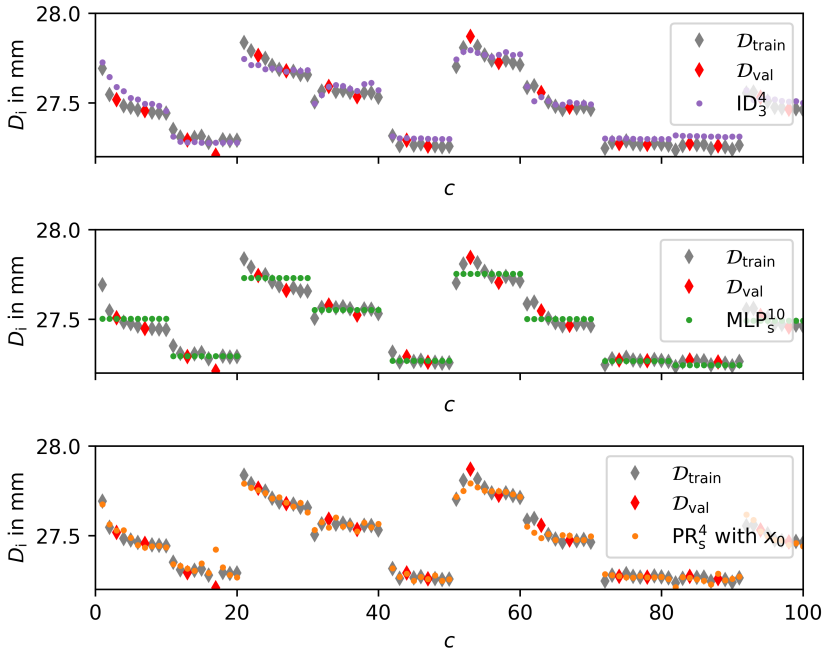

FIGURE 1.21 Prediction of ID_3^4 (top), MLP_s^{10} (middle) and PR_s^4 with x_0 (bottom) on $\mathcal{D}_{\text{train}}$ and $\mathcal{D}_{\text{val}}$.

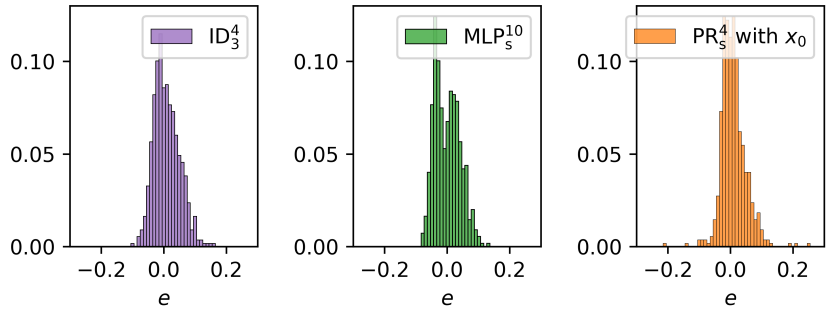

FIGURE 1.22 Prediction error e of ID_3^4 (left), MLP_s^{10} (middle) and PR_s^4 with x_0 (right) on $\mathcal{D}_{\mathrm{val}}$.

prediction errors in Fig. 1.22. PR_s^4 with x_0 has more prediction errors that exceed ± 0.1 mm compared to MLP_s^{10}. These larger errors have a disproportionate effect since the BFR is quadratic in e. It should also be mentioned, that the prediction errors of all three models are not normally distributed according to a Shapiro-Wilk test. Fig. 1.23 clearly shows, that within three distinguishable clusters the prediction error slightly increases with increasing D_i. I.e. smaller D_i tend to be overestimated while larger D_i tend to be underestimated within these clusters. Hence there exists some, albeit minor, deterministic relation none of the models was able to capture, either because the model is not complex enough or missing model inputs. A phenomenon that might be difficult to model even for the most complex considered candidate structures is the change in monotonicity that can be observed for neighboring setpoints, e.g. cycles 21-30 and 51-60 in Fig. 1.16a. During both experiments cavity temperature increases steadily with every cycle. During cycles 21-30 D_i decreases monotonously, as is expected since thermal expansion causes the cavity to shrink. During cycles 51-60 however, D_i increases sharply during the first few cycles before it decreases and approaches a constant value. These changes in monotonicity can be observed for setpoints directly adjacent in the setpoint space, a nonlinear behavior that is difficult to capture. Considered additional model inputs were ambient temperature, ambient humidity and the number of completed production cycles during that day (as a measure for the duration of continuous production of the machine). None of these inputs improved predictive performance.

1.6 CONCLUSIONS & OUTLOOK

1.6.1 Conclusions

The purpose of this work was to provide and implement a framework for the development of a Digital Twin of an industrial plastic injection molding machine. Therefore, a system for process data acquisition was developed, which records

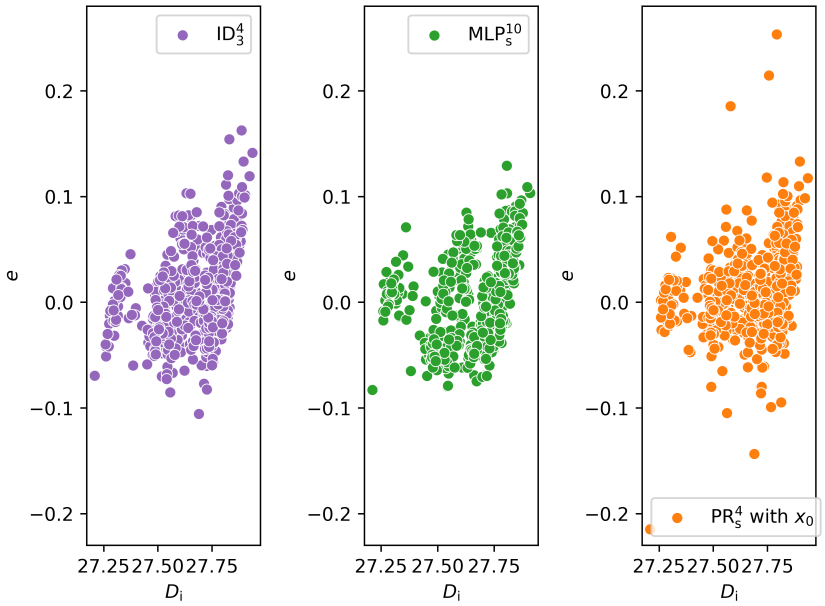

FIGURE 1.23 Prediction error e vs. D_i of ID$_3^4$ (left), MLP$_s^{10}$ (middle) and PR$_s^4$ with x_0 (right) on $\mathcal{D}_{val}$.

the process data (single values and trajectories) cycle-related via the OPC-UA interface of the IM machine in series production. An additional temperature and pressure sensor was installed in the cavity of the injection mold for the analysis of quality-relevant state variables. It was shown that the frequency of the recorded process variables is high enough that all information contained in the trajectories is available. For the development of a Digital Twin, quality variables must be recorded in-line in addition to the process variables. For this purpose, the quality data of the manufactured tamper-evident closure were recorded during the following process cycle within the cycle time. The weight was recorded with the aid of a laboratory scale and the dimensional accuracy (diameter and distances) was measured by a digital measuring projector. By applying a design of experiment (face centered central composite design), the described experimental setup was used to sample a process window as large as possible for training different models. Subsequently, the crucial aspect of finding an appropriate model representation of the plastic injection molding process for part quality prediction was investigated.

Various static and dynamic modeling approaches were compared in a case study. The case study revealed, that there is a substantial amount of variation in part quality not only between but also within a certain process setpoint. A proposed internal dynamics approach for part quality prediction from raw process

variable measurements was able to explain more than 90 % of the variance in the dataset. However, a static polynomial model considering the process setpoint and process variable measurements at thee beginning of a cycle performed almost as well. Since the effort of training the latter is considerably less, they have been found to provide the best trade-off in this specific case study. From the point of view of the practitioner it is certainly most welcome that the easiest to implement and fastest to estimate model approach yields highly competitive prediction models.

1.6.2 Outlook

Future work will cover the estimation of quality models for more involved quantities, such as mechanical properties of the produced part. It is suspected that the quantities considered in this case study, i.e. part weight and geometric properties, are influenced by the actual course of the process to little extent. As long as the cavity is filled properly and its volume remains constant (due to thermal expansion) these quantities will vary little. The proposed internal dynamics approach is expected to have an advantage over static approaches, if the course of the process influences the considered quality variable considerably. This is expected to be the case with mechanical properties, such as a parts tensile strength, where especially the evolution of the temperature is a significant factor.

In future, the Digital Twin will also be employed for quality optimization. The static models estimated in this work are in principal already fit for this purpose. In order to take into account the effect of creeping disturbances like machine wear and tear, as well as changes in ambient temperature the parameters should be re-estimated or estimated recursively once the prediction error increases. As mentioned above, a dynamic process model, from which in conjuncture with the dynamic quality model the optimal process setpoints can then be inferred, needs to be estimated to complete the dynamical Digital Twin. This aspect will be covered in future work as well. Although, based on the experience gained from the case study conducted in this work an incremental increase in predictive performance is expected at best.

Finally, in order to truly close the quality optimization loop, the optimal machine setpoints need to be applied automatically to the machine. Up to now producers only have reading access to the nodes in the OPC-UA address space of the injection molding machine. So in order to achieve autonomous smart manufacturing writing permission to the machine has to be enabled by injection molding machine manufacturers.

Bibliography

[1] *VDI-Statusreport Februar 2019: Industrie 4.0 in Spritzgießunternehmen*. `https://www.vdi.de/ueber-uns/presse/publikationen/`

details/vdi-statusreport-industrie-40-in-spritzgiessunternehmen. Accessed: 29.07.2020.

[2] H.-P. Heim. *Specialized injection molding techniques*. William Andrew, 2015.

[3] V. Goodship. *Injection Moulding: A Practical Guide*. De Gruyter, 2020.

[4] A.M. Merrill. *Plastics Technology*. Bd. 1. Rubber/Automotive Division of Hartman Communications, Incorporated, 1955.

[5] K.-M. Tsai, C.-Y. Hsieh, and W.-C. Lo. "A study of the effects of process parameters for injection molding on surface quality of optical lenses". In: *Journal of Materials Processing Technology* 209.7 (2009), pp. 3469–3477. ISSN: 0924-0136. DOI: https://doi.org/10.1016/j.jmatprotec.2008.08.006.

[6] M. Rohde et al. "Influence of Processing Parameters on the Fiber Length and Impact Properties of Injection Molded Long Glass Fiber Reinforced Polypropylene". In: *International Polymer Processing* 26.3 (2011), pp. 292–303. DOI: doi:10.3139/217.2442.

[7] M. Mohan, M.N.M. Ansari, and R. A. Shanks. "Review on the Effects of Process Parameters on Strength, Shrinkage, and Warpage of Injection Molding Plastic Component". In: *Polymer-Plastics Technology and Engineering* 56.1 (2017), pp. 1–12. DOI: 10.1080/03602559.2015.1132466.

[8] E. Farotti and M. Natalini. "Injection molding. Influence of process parameters on mechanical properties of polypropylene polymer. A first study." In: *Procedia Structural Integrity* 8 (2018), pp. 256–264. DOI: https://doi.org/10.1016/j.prostr.2017.12.027.

[9] P. Sälzer, M. Feldmann, and H.-P. Heim. "Wood-Polypropylene Composites: Influence of Processing on the Particle Shape and Size in Correlation with the Mechanical Properties Using Dynamic Image Analysis". In: *International Polymer Processing* 33.5 (2018), pp. 677–687. DOI: doi:10.3139/217.3446.

[10] A. Tellaeche and R. Arana. "Machine learning algorithms for quality control in plastic molding industry". In: *2013 IEEE 18th Conference on Emerging Technologies & Factory Automation (ETFA)*. 2013, pp. 1–4. DOI: 10.1109/ETFA.2013.6648103.

[11] O. Ogorodnyk et al. "Application of Machine Learning Methods for Prediction of Parts Quality in Thermoplastics Injection Molding". In: *Advanced Manufacturing and Automation VIII*. Ed. by Kesheng Wang et al. Singapore: Springer Singapore, 2019, pp. 237–244.

[12] F. Finkeldey et al. “Learning quality characteristics for plastic injection molding processes using a combination of simulated and measured data”. In: *Journal of Manufacturing Processes* 60 (2020), pp. 134–143. ISSN: 1526-6125. DOI: https://doi.org/10.1016/j.jmapro.2020.10.028.

[13] H. Jung et al. “Application of Machine Learning Techniques in Injection Molding Quality Prediction: Implications on Sustainable Manufacturing Industry”. In: *Sustainability* 13.8 (2021), p. 4120.

[14] S. K. Selvaraj et al. “A review on machine learning models in injection molding machines”. In: *Advances in Materials Science and Engineering* 2022 (2022). DOI: https://doi.org/10.1155/2022/1949061.

[15] Y. Lu et al. “Digital Twin-driven smart manufacturing: Connotation, reference model, applications and research issues”. In: *Robotics and Computer-Integrated Manufacturing* 61 (2020), p. 101837.

[16] P. Bibow et al. “Model-driven development of a digital twin for injection molding”. In: *International Conference on Advanced Information Systems Engineering*. Springer. 2020, pp. 85–100.

[17] F. Tao and M. Zhang. “Digital twin shop-floor: a new shop-floor paradigm towards smart manufacturing”. In: *Ieee Access* 5 (2017), pp. 20418–20427.

[18] S. Stemmler et al. “Cross-phase model-based predictive cavity pressure control in injection molding”. In: *2019 IEEE Conference on Control Technology and Applications (CCTA)*. IEEE. 2019, pp. 360–367.

[19] C. Hopmann et al. “Self-optimizing injection molding based on iterative learning cavity pressure control”. In: *Production Engineering* 11.2 (2017), pp. 97–106.

[20] S. Stemmler et al. “Quality control in injection molding based on norm-optimal iterative learning cavity pressure control”. In: *IFAC-PapersOnLine* 53.2 (2020), pp. 10380–10387.

[21] H. Karbasi and H. Reiser. “Smart mold: Real-time in-cavity data acquisition”. In: *First Annual Technical Showcase & Third Annual Workshop, Canada*. Citeseer. 2006.

[22] H. S. Park, D. X. Phuong, and S. Kumar. “AI based injection molding process for consistent product quality”. In: *Procedia Manufacturing* 28 (2019), pp. 102–106.

[23] C. Hopmann, A. Reßmann, and J. Heinisch. “Influence on product quality by pvT-optimised processing in injection compression molding”. In: *International Polymer Processing* 31.2 (2016), pp. 156–165.

[24] K.-C. Ke and M.-S. Huang. “Quality Prediction for Injection Molding by Using a Multilayer Perceptron Neural Network”. In: *Polymers* 12.8 (2020), p. 1812.

[25] P. Zhao et al. "A nondestructive online method for monitoring the injection molding process by collecting and analyzing machine running data". In: *The International Journal of Advanced Manufacturing Technology* 72.5 (2014), pp. 765–777.

[26] B. Silva, J. Sousa, and G. Alenya. "Data Acquisition and Monitoring System for Legacy Injection Machines". In: *2021 IEEE International Conference on Computational Intelligence and Virtual Environments for Measurement Systems and Applications (CIVEMSA)*. IEEE. 2021, pp. 1–6.

[27] A. Martins et al. "An approach to integrating manufacturing data from legacy Injection Moulding Machines using OPC UA". In: *37th International Manufacturing Conference (IMC37)*. 2021.

[28] EUROMAP. *EUROMAP 83 – OPC UA interfaces for plastics and rubber machinery – General Type definitions*. June 2021. URL: https://www.euromap.org/euromap83.

[29] EUROMAP. *EUROMAP 77 – OPC UA interfaces for plastics and rubber machinery – Data exchange between injection moulding machines and MES*. June 2020. URL: https://www.euromap.org/euromap77.

[30] X. Tang et al. "Final quality prediction for multi-phase batch process based on phase cumulative product quality model". In: *Transactions of the Institute of Measurement and Control* 36.5 (2014), pp. 696–708.

[31] W.-C. Chen et al. "A neural network-based approach for dynamic quality prediction in a plastic injection molding process". In: *Expert systems with Applications* 35.3 (2008), pp. 843–849.

[32] W.-C. Chen and D. Kurniawan. "Process parameters optimization for multiple quality characteristics in plastic injection molding using Taguchi method, BPNN, GA, and hybrid PSO-GA". In: *IJPEM* 15.8 (2014), pp. 1583–1593.

[33] J. Wan, O. Marjanovic, and B. Lennox. "Uneven batch data alignment with application to the control of batch end-product quality". In: *ISA transactions* 53.2 (2014), pp. 584–590.

[34] W. Michaeli and J. Gruber. "Prozessführung beim Spritzgießen–direkte Regelung des Werkzeuginnendrucks steigert die Reproduzierbarkeit". In: *Zeitschrift Kunststofftechnik* 6 (2005).

[35] Y. Yao and F. Gao. "A survey on multistage/multiphase statistical modeling methods for batch processes". In: *Annual Reviews in Control* 33.2 (2009), pp. 172–183.

[36] F. A. Gers, J. Schmidhuber, and F. Cummins. "Learning to forget: Continual prediction with LSTM". In: *Neural computation* 12.10 (2000), pp. 2451–2471.

[37] Alexander Rehmer and Andras Kroll. “The effect of the forget gate on bifurcation boundaries and dynamics in Recurrent Neural Networks and its implications for gradient-based optimization”. In: *Preprints of the International Joint Conference on Neural Networks (IJCNN 2022)*. accepted. Padua, Italy, 2022.

[38] Julian Heinisch, Yannik Lockner, and Christian Hopmann. “Comparison of design of experiment methods for modeling injection molding experiments using artificial neural networks”. In: *Journal of Manufacturing Processes* 61 (2021), pp. 357–368.

[39] J. A. E. Andersson et al. “CasADi – A software framework for nonlinear optimization and optimal control”. In: *Mathematical Programming Computation* (2018).

[40] A. Wächter and L. T. Biegler. “On the implementation of an interior-point filter line-search algorithm for large-scale nonlinear programming”. In: *Mathematical programming* 106.1 (2006), pp. 25–57.

Chapter 2

Chapter Title[1]

Chapter Subtitle

Firstname Surname[a,b] and Firstname Surname[b]
[a]*Short Address,* [b]*Long Address*

Chapter Points

- The ends of words and sentences are marked by spaces. It doesn't matter how many spaces you type; one is as good as 100. The end of a line counts as a space.
- The ends of words and sentences are marked by spaces. It doesn't matter how many spaces you type; one is as good as 100. The end of a line counts as a space.

The ends of words and sentences are marked by spaces. It doesn't matter how many spaces you type; one is as good as 100. The end of a line counts as a space. The ends of words and sentences are marked by spaces. It doesn't matter how many spaces you type; one is as good as 100. The end of a line counts as a space.

Name

2.1 SECTION TITLE

1. This is chapter footnote

Appendix A

Appendix title

Appendix B

Appendix title